

## Article

# An Integrated Approach for Evaluating the Restoration of the Salinity Gradient in Transitional Waters: Monitoring and Numerical Modeling in the Life Lagoon Refresh Case Study

Alessandra Feola <sup>1,\*</sup>, Emanuele Ponis <sup>1</sup>, Michele Cornello <sup>1</sup>, Rossella Boscolo Brusà <sup>1</sup>, Federica Cacciatore <sup>1</sup>, Federica Oselladore <sup>1</sup>, Bruno Matticchio <sup>2</sup>, Devis Canesso <sup>2</sup>, Simone Sponga <sup>2</sup>, Paolo Peretti <sup>2</sup>, Matteo Lizier <sup>3</sup>, Luigi Maniero <sup>4</sup>, Valerio Volpe <sup>4</sup>, Adriano Sfriso <sup>5</sup>, Maurizio Ferla <sup>1</sup> and Andrea Bonometto <sup>1</sup>

**Citation:** Feola, A.; Ponis, E.; Cornello, M.; Boscolo Brusà, R.; Cacciatore, F.; Oselladore, F.; Matticchio, B.; Canesso, D.; Sponga, S.; Peretti, P.; et al. An Integrated Approach for Evaluating the Restoration of the Salinity Gradient in Transitional Waters: Monitoring and Numerical Modeling in the Life Lagoon Refresh Case Study. *Environments* **2022**, *9*, 31. <https://doi.org/10.3390/environments9030031>

Academic Editor: Paul C. Sutton

Received: 27 January 2022

Accepted: 25 February 2022

Published: 1 March 2022

**Publisher's Note:** MDPI stays neutral with regard to jurisdictional claims in published maps and institutional affiliations.



**Copyright:** © 2022 by the authors. Licensee MDPI, Basel, Switzerland. This article is an open access article distributed under the terms and conditions of the Creative Commons Attribution (CC BY) license (<https://creativecommons.org/licenses/by/4.0/>).

<sup>1</sup> ISPRA, Italian National Institute for Environmental Protection and Research, Località Brondolo, 5-30015 Chioggia, Italy; emanuele.ponis@isprambiente.it (E.P.); michele.cornello@isprambiente.it (M.C.); rossella.boscolo@isprambiente.it (R.B.B.); federica.cacciatore@isprambiente.it (F.C.); federica.oselladore@isprambiente.it (F.O.); maurizio.ferla@isprambiente.it (M.F.); andrea.bonometto@isprambiente.it (A.B.)

<sup>2</sup> IPROS Ingegneria Ambientale S.r.l., Corso del Popolo, 35131 Padua, Italy; matticchio@ipros.it (B.M.); canesso@ipros.it (D.C.); sponga@ipros.it (S.S.); peretti@ipros.it (P.P.)

<sup>3</sup> Direction for Special Projects for Venice-Veneto Region, Calle Priuli—Cannaregio, 99-30121 Venice, Italy; matteo.lizier@regione.veneto.it

<sup>4</sup> Interregional Superintendency for Public Works in Veneto—Trentino Alto Adige—Friuli Venezia Giulia, San Polo, 19-30125 Venice, Italy; luigi.maniero@mit.gov.it (L.M.); valerio.volpe@mit.gov.it (V.V.)

<sup>5</sup> Department of Environmental Sciences, Informatics and Statistics, University Ca' Foscari Venice, Via Torino 155, 30172 Mestre, Italy; sfrisoad@unive.it

\* Correspondence: alessandra.feola@isprambiente.it; Tel.: +39-347-1814149

**Abstract:** Large lagoons usually show a salinity gradient due to fresh water tributaries with inner areas characterized by lower mean values and higher fluctuation of salinity than seawater-dominated areas. In the Venice Lagoon, this ecotonal environment, characterized in the past by oligo-mesohaline waters and large intertidal areas vegetated by reedbeds, was greatly reduced by historical human environmental modifications, including the diversion of main rivers outside the Venice Lagoon. The reduction of the fresh water inputs caused a marinization of the lagoon, with an increase in salinity and the loss of the related habitats, biodiversity, and ecosystem services. To counteract this issue, conservation actions, such as the construction of hydraulic infrastructures for the introduction and the regulation of a fresh water flow, can be implemented. The effectiveness of these actions can be preliminarily investigated and then verified through the combined implementation of environmental monitoring and numerical modeling. Through the results of the monitoring activity carried out in Venice Lagoon in the framework of the Life Lagoon Refresh (LIFE16NAT/IT/000663) project, the study of salinity is shown to be a successful and robust combination of different types of monitoring techniques. In particular, the characterization of salinity is obtained by the acquisition of continuous data, field campaigns, and numerical modeling.

**Keywords:** transitional waters; integrated approach; numerical modeling; restoration; monitoring; salinity gradient; fresh water; life project

## 1. Introduction

Coastal lagoons are ecotones between marine and terrestrial environments, receiving variable amounts of fresh water. Along the Mediterranean coastline, there are more than 400 coastal lagoons, covering a wide range of hydrological and biological characteristics [1,2]. Mediterranean lagoons are usually shallow water bodies, and, due to their geomorphological and hydrological characteristics, environmental conditions in them

undergo frequent fluctuations on a spatial and seasonal basis [3]. These are heterogeneous and complex systems, characterized by different physical and environmental gradients, involving salinity, marine water renewal (e.g., residence time), nutrients, turbidity and sediment structure, whose magnitude and direction depend mainly on river or tidal energy [4]. The distribution of biological communities in transitional waters is driven by multiple environmental factors, including salinity [5], which affects the composition and abundance of fish fauna [6], benthic flora and fauna [7] and saltmarsh vegetation [8].

Salinity conditions are related to a complex interaction between different hydrological processes that involve discharge of fresh water, tidal regime and the exchanges with the sea, precipitation, interaction with the atmosphere (e.g., heat flux, evaporation rates) and wind-driven forces, which vary over a wide range of time-scales and that become relevant for really shallow waters, resulting in strong daily and seasonal variability [9,10]. All these drivers contribute to the high diversity in terms of salinity conditions between Mediterranean lagoons, ranging from oligohaline to hyperhaline waters [11].

Despite this high diversity, it is possible to identify some common patterns. In particular, large lagoons usually show a salinity gradient due to fresh water tributaries that exhibit estuarine features in the proximity of their lagoonal mouths [12], characterized by lower mean values and higher fluctuation of salinity than seawater-dominated areas [13–15].

In the Venice Lagoon, this ecotonal environment typical of the inner areas, characterized in the past by oligo-mesohaline waters and large intertidal areas vegetated by reedbeds, has been greatly reduced by historical human environmental modifications, among which the diversion outside the Venice Lagoon of main rivers such as Brenta, Bacchiglione, Sile and Piave (Figure 1; [16]).

The reduction of the fresh water inputs and the related sediment supply, together with other concurrent factors such as the construction of inlet jetties and the deepening the lagoon inlets (19th–20th century), the excavation of large navigation canals (20th century), increasing of the lagoon depth due to the combined effect of subsidence and eustatism, caused a marinization of the lagoon, with a progressively increase in salinity from average values of 10–14 documented in 1926–1928 to the current values close to 30 [16–18].

The problem of managing the hydraulic aspects for lagoons has been studied for a long time worldwide. These studies include the description of lagoon physics, how hydraulics are linked to lagoon ecology and productivity, how lagoons might be expected to respond to hydraulic alterations and protocol for physical investigations [19].

The restoration of both abiotic and biotic components of transitional water ecosystems is recognized as a strategic approach to both enhance the ecological status of degraded ecosystems and tackle the loss of biodiversity. Ecological Engineering is increasingly used to re-create and restore ecosystems degraded by previous human activities. In this context, the so-called Ecohydrological approach [20] aims at restoring natural processes, especially regarding water and sediment flows, by recovering the suitable conditions for habitats and species.

The Life Lagoon Refresh project, started in September 2017 and lasting for five years, planned the re-introduction of a fresh water flow into the lagoon, to partially recover the oligo-mesohaline conditions suitable for the reedbed colonization [21]. This low-salinity habitat, typical of the buffer areas between lagoon and mainland, provides valuable and diversified ecosystem services (see [22] and references therein), including water purification, nursery functions and breeding, feeding or refuge habitat for several fish and bird species of commercial and conservation interest.

The core action of the project was the diversion of a fresh water flow of approximately  $1000 \text{ l s}^{-1}$  from the Sile River into the Venice Lagoon. Other measures included the implementation of structures made by biodegradable geotextile, properly arranged to slow down the fresh water dispersion, and permitting the planting of clumps and

rhizomes of *Phragmites australis* (Cav.) Trin. ex Steud, to accelerate the development of the reedbeds.

The objective of saline gradient recovery was quantified in an expected change from a salinity value of 30 to less than 5 in at least 5 ha, less than 15 in at least 25 ha and less than 25 in at least 70 ha.

We applied an adaptive management by:

1. quantitative definition of the project objectives through numerical modeling, design of the hydraulic works and identification of the proper fresh water discharge necessary to achieve the objectives;
2. implementation of the integrated analysis approach through monitoring and validated numerical modeling;
3. assessment of results and verification of compliance of management objectives;
4. completion of conservation actions with a step-by-step approach supported by monitoring and modeling results.

During the different phases of this adaptive management approach, an intensive monitoring and modeling activity was carried out to support the assessment of the success of the implemented measures and of the identified mitigation actions. In microtidal lagoons, this monitoring activity needs to integrate different strategies able to capture, with the best resolution in time and space, variations of water levels, flows and salinity that are often encountered [11].

In this context, tools such as numerical models can usefully integrate observations and measurements, to manage the variability in time and space of descriptors [15], providing a more holistic description of the physical, chemical and biological dynamics [13].

Through the results of the monitoring activity carried out in Venice Lagoon in the framework of the Life Lagoon Refresh project, this paper illustrates how the study of salinity in estuarine environment can become successful and robust combining different types of monitoring techniques.

In particular, the characterization in time and space of salinity variations, performed before and after the conservation actions, was obtained by the integration of three different tools: moored salinity probes that allow the acquisition, in fixed positions, of continuous measured data; field campaigns with CTD profilers that allow the acquisition of instantaneous/spatially distributed measured data; the implementation of numerical modeling that allows the simulation of variations in space and time. Arguments for and against the use of the different tools and measures and the importance of an integrated approach, that effectively combines measured and modeled data, are discussed.

## 2. Materials and Methods

### 2.1. Study Area and Project Details

The Venice Lagoon is one of the largest coastal lagoons in the Mediterranean Sea (approximately 550 km<sup>2</sup>). It is connected to the Northern Adriatic Sea by three inlets, and experiences microtidal conditions with a tidal range of  $\pm 0.50$  m during spring tides [23]. The lagoon basin is mainly composed by shallow water areas (average depth of 1.2 m) intersected by a network of deeper channels leading inwards from the inlets and branching inside each sub-basin [6,24–26].

The lagoon is also characterized by several fresh water inputs from the drainage basin, the most consistent of which are located in the northern sub-basin [15]. The current supply of fresh water from the catchment area is about 30 m<sup>3</sup>/s for the entire lagoon and about 17 m<sup>3</sup>/s for the Northern Lagoon [17]. Most of the fresh waters that originally flowed in the Northern Lagoon, through the Sile River and other minor rivers, were diverted into the abandoned riverbed of Piave River with the construction, on the northeastern edge of the lagoon, of the “Taglio del Sile” canal (1683).

Along the Sile river embankment, close to the area of the project, a spillway was built after the extreme event of 1966 to protect the town of Jesolo, located downstream, from the risk of flooding. In addition to the new fresh water input implemented by the Project, during significant overflow events, a considerable volume of fresh water enters the lagoon through this spillway, with peaks of flow rates of tens of  $\text{m}^3/\text{s}$ . Between 2002 and 2017, about nine significant overflow events were recorded per year, with an average volume of water spilled into the lagoon of about 460,000  $\text{m}^3$  per event.

The Life Lagoon Refresh project foresees different conservation actions that consist of fresh water diversion in the Sile river embankment, morphological reconstruction and reedbed transplantation in the lagoonal area of 70 ha located in front of the hydraulic opera (Intervention area) and aquatic angiosperm transplantation in about 1900 ha (Project Site), as reported in Figure 1.

The intervention area is a shallow, inner portion of the northern sub-basin, characterized by an average depth of 60 cm, by the presence of residues of saltmarshes, mainly eroded by the wind action and the related wave action, and by the almost complete absence of channels that makes the navigation in the area particularly difficult.

It is characterized by high-water residence times ( $>20$  days [24]) and euhaline conditions, with salinity levels often higher than 30 [15,27]. From a technical point of view, the area was chosen because it was close to the course of the Sile River, with flow rates and water quality adequate to allow the deviation of a part of the flow into the lagoon.

The fresh water inflow from the Sile River to the lagoon is permitted by a hydraulic infrastructure, realized between 08/2019 and 02/2020 within the project, consisting in a canal for intake from Sile River, a crossing section of the embankment made by two parallel pipes (diameter of 0.8 m) equipped with sluice gates to regulate the flow rate and a return canal in the lagoon. The fresh water occurs by gravity, according to the difference between the river level and the tidal level in the lagoon.

The structure was equipped with two flow meters providing remotely accessible data in real time. After the completion of the infrastructure (post operam phase), the fresh water inflow was gradually increased starting from approx. 300  $\text{ls}^{-1}$  in May 2020 up to 1000  $\text{ls}^{-1}$  in February 2021.

The morphological works were carried out using modular biodegradable elements, positioned on the shallow lagoon bottom to slow down the dispersion of fresh water introduced into the lagoon and to allow the establishment of a suitable substrate for the development of reedbeds.

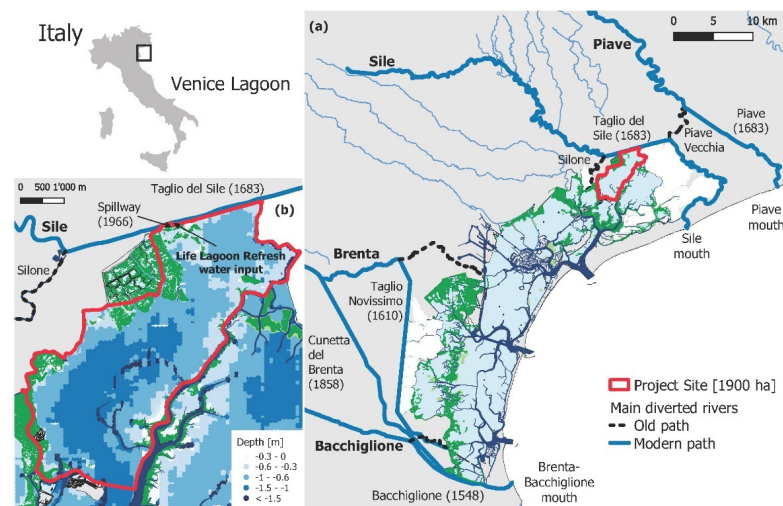


**Figure 1.** (a) A map of the Venice Lagoon with main rivers (Bacchiglione and Brenta in the south, Sile and Piave in the north) diverted during historical human environmental modifications [16]; (b) project site and the new fresh water input realized by the Life Lagoon Refresh project.



## 2.2. Moored Probes

To investigate the variability in time of salinity in fixed positions, three moored probes were installed. In particular, continuous measures were acquired using instrumented buoys (IJINUS, Claire Group, Mellac, France) equipped with conductivity (graphite and platinum electrodes) and temperature sensors. Salinity was calculated automatically by the probe using the UNESCO algorithm [28]. The instrumented buoy is about 50 cm long (without the antenna) and it is adequate for the monitoring of shallow waters subjected to microtidal cycle. The instrumented buoys were anchored using a ballast and the measures were acquired at a constant depth of approx. 25–30 cm from the water surface. Data were continuously acquired with a frequency of 10 min. An internal datalogger stored the data and a GSM/GPRS system was used for their daily transmission. The installed probes were regularly maintained and cleaned in situ to ensure the quality of the collected data, with a frequency of 15–30 days, according to the seasonal conditions.

The strategy of salinity monitoring was modulated according to the progress of the operative state of the project. In particular, two phases were identified: one before (ante operam) and one after (post operam) the start of the fresh water inflow by the hydraulic infrastructure. The three buoys are located along a transect at increasing distances from the inflow location: P1 close to the hydraulic infrastructure, P3 outside the morphological structure, considered to be a reference location, and P2 located in an intermediate position. P3b is an additional position used in a short period to investigate suitable condition for reedbed in term of mean salinity. The localization of the moored stations is shown in Figure 2.

During the ante operam phase, salinity was monitored over a period of one year (May 2019–April 2020) using P2 and P3 probes. During the post operam phase, starting from May 2020 with fresh water of  $300 \text{ ls}^{-1}$  and gradually increased up to  $1000 \text{ ls}^{-1}$ , salinity was monitored also in P1.

All data transmitted by the buoys were collected in an FTP server and daily incorporated in a specific database, which contains meteo-marine data implemented by ISPRA including, among others, an estimation of the tidal level in different parts of Venice Lagoon.

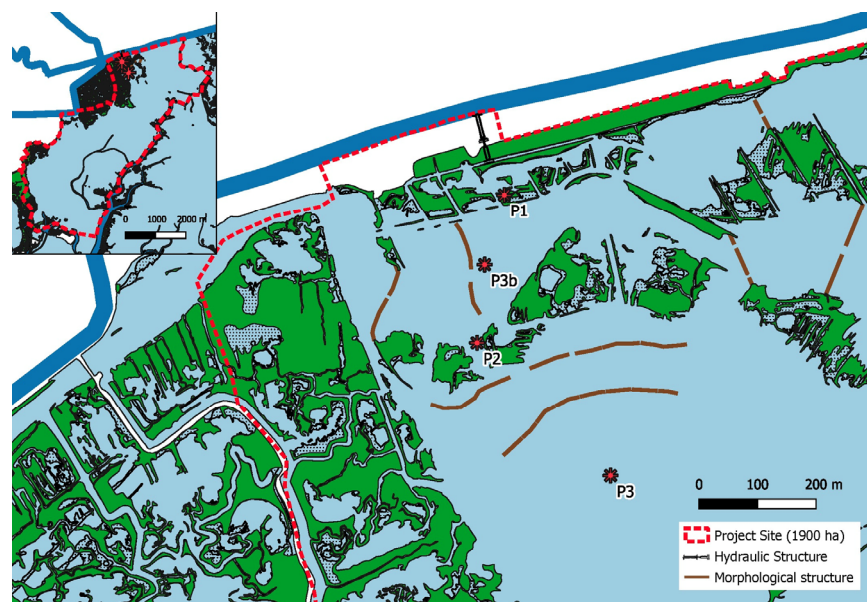


**Figure 2.** Moored probes: location along a transect within the area in front of Hydraulic and Morphological structures. P1: close to the hydraulic infrastructure; P2: located in an intermediate position; and P3: in a third site outside the morphological structure, considered to be a reference location. P3b position, to investigate suitable condition for reedbed, is also reported.

Data were processed to eliminate spurious values due to momentary air exposition of the sensors during very low tides as well as to instrumental issues. A two-step process was chosen. First salinity values below 0.1 and over 41 were eliminated. The second step was to calculate the Z-score value into a mobile window of 6 h (half of the tide cycle, 37 values):

$$Z_{\text{score}} = \frac{x - \mu}{\sigma} \quad (1)$$

with  $\mu$  mean value and  $\sigma$  standard deviation within the mobile window. Values with associated Z-score bigger than 1.96 or smaller than -1.96, corresponding to the 97.5 percentile point of a standard normal distribution, were eliminated.

After the cleaning process, data were elaborated to get main daily statistics as mean, median, quartiles. The percentage of time with salinity values below 5-15-25, chosen as quantitative objectives for project goals, was calculated. In particular, the value of 15 is considered a threshold for reedbed suitability [29].

Timeseries were also evaluated in relation to tidal level, fresh water discharge and river overflow.

### 2.3. CTD Profiles

Different field campaigns performed to acquire CTD (Conductivity, Temperature, Depth) profiles were planned, to investigate the instantaneous/spatially distributed characterization of salinity within the area of interest.

A combined strategy with two boats and respective equipment allowed to acquire data simultaneously at a local and large scale. In particular, at the local scale a detailed grid of 25 vertical profiles of measures was used to evaluate local effects close to the intervention area (about 1.3 km<sup>2</sup>), while four transects were investigated with vertical profile collection at a regular distance of 350 m to evaluate the salinity at a larger scale (Figure 3).

The multiparameter probe used for the large-scale sampling is an Ocean Seven 316Plus model by Idronaut Srl (Brugherio (MB), Italy), equipped with the following sensors: pressure, conductivity and temperature. Pressure sensor accuracy and resolution are 0.02 dbar, and 0.008 dbar, respectively; conductivity sensor accuracy and resolution are 0.003 mS/cm and 0.00025 mS/cm, respectively; temperature sensor accuracy and resolution are 0.003 °C and 0.0002 °C, respectively. Time acquisition was set at 20 Hz and data are stored in an internal non-volatile memory. Data were formerly processed with Idronaut software REDAS-5.

A SonTek CastAway-CTD multiparameter probe equipped with pressure, conductivity and temperature sensors was used for the local scale sampling. It also had an internal GPS receiver, used to associate the field position with each cast. The acquisition sample rate was set at 5 Hz, pressure sensor accuracy is  $\pm 0.25\%$  and resolution was 0.01 dbar and conductivity sensor accuracy is  $0.25\% \pm 0.005$  mS/cm and resolution was 0.001 mS/cm. Temperature sensor accuracy and resolution were  $\pm 0.05$  °C and 0.001 C, respectively.

During the ante operam phase, salinity was monitored in 2018 over two seasonal campaigns (spring, autumn) at different tidal conditions (spring-neap tide).

During the post operam phase, the fresh water was gradually increased starting from 300 ls<sup>-1</sup> in May 2020 up to 1000 ls<sup>-1</sup> in February 2021, and the distribution of fresh water was monitored on different occasions. Details are summarized in Table 1.

In this paper, only spring tidal conditions are evaluated and compared before and after the realization of the conservation actions.

In each campaign, the distribution of salinity was possibly investigated in two different tidal conditions to evaluate the minimum and maximum diffusion as a function of tidal phase (flood/ebb).

The vertical profiles, acquired with a centimetric precision and post-processed with a vertical resolution of 5 cm, were interpolated using a Kriging method giving an instantaneous characterization of the spatial (planimetric and vertical) distribution of salinity in

terms of mean value within a surface layer of about 30 cm and mean value along the entire water column.

The spatial interpolation using the Kriging method was carried out with Esri ArcMap 10.3.1 and resulted in a geotiff raster map per dataset with a cell resolution of 2 m.

From maps of the spatial distribution of salinity, obtained for each campaign and each investigated tidal condition, two transects were extracted to verify the gradient of salinity between the lagoon side and the land side.

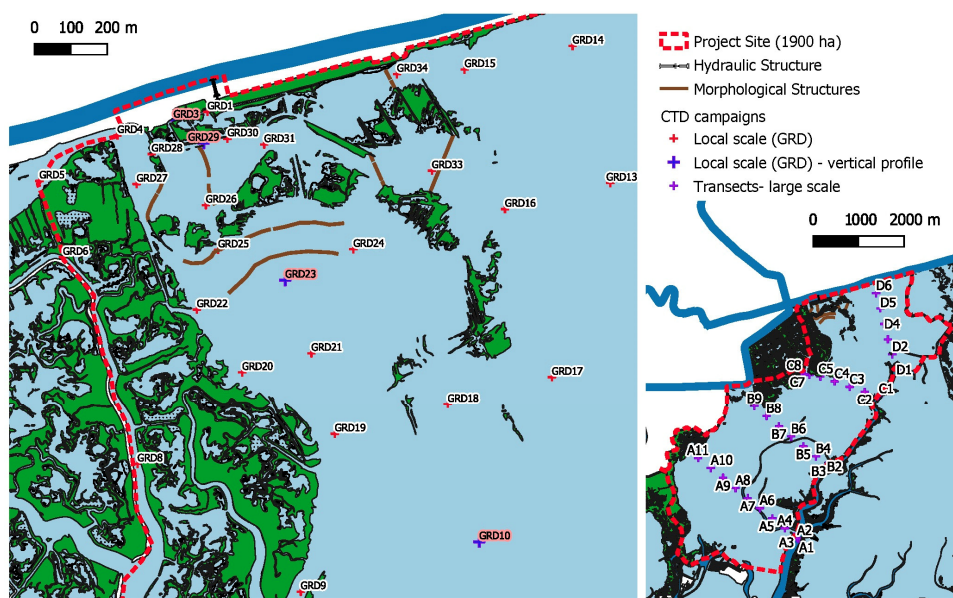


**Figure 3.** CTD campaigns: local and large scale strategies. Points with information relative to the complete vertical profile are also indicated.

**Table 1.** CTD campaigns before and after the opening of the fresh water flow. Mean tide values are evaluated according to the nearest ISPRA’s meteo-mareographic station located in Grassabò area. Values of tidal level are referred to m a.s.l. and they are averaged values within each timewindow. (\*) Campaigns considered for this study.

Phase	CTD Campaign	Investigated Tidal Condition	Discharge
Ante operam—no flow	16 April 2018 (*)	Spring tide (flood tide with a mean value of 0.05 m a.s.l. between 8:25–12:00 summer time, ebb tide with a mean value of 0.25 between 14:10–16:15 summer time)	0 ls <sup>-1</sup>
	18 November 2018 (local scale)	Neap tide (Local scale: low tide unique phase with a mean value of 0.15 m a.s.l. between 10:00–16:30 summer time. Large scale: high tide unique phase with a mean value of 0.44 m a.s.l. between 12:00–16:30 standard time)	0 ls <sup>-1</sup>
	31 October 2018 (large scale)		
Post operam—fresh water flow	23 June 2020 (*)	Spring tide (beginning high tide with a mean value of −0.15 m a.s.l. between 9:20–12:10 summer time, high tide with a value of 0.30 m a.s.l. between 14:40–17:00 summer time)	300 ls <sup>-1</sup>
	28 January 2021	Spring tide (beginning low tide with a mean value of 0.65 m a.s.l. between 11:00–13:30 standard time, ending low tide with a value of 0.15 m a.s.l. between 14:40–17:00 standard time)	500 ls <sup>-1</sup>
	26 February 2021 (*)	Spring tide Local scale: unique phase with flow tide, mean value of 0.16 m a.s.l. between 9:30–12:30 standard time	1000 ls <sup>-1</sup>
	10 June 2021 (*)	Spring tide	1000 ls <sup>-1</sup>

	(unique phase with ebb tide, mean value of 0.20 m a.s.l. between 14:00–16:00 summer time)	
	Neap tide	
15 November 2021	(Local scale: low tide unique phase with a mean value of 0.23 m a.s.l. between 15:00–16:10 summer time)	1000 $1s^{-1}$

#### 2.4. Numerical Modeling

A numerical hydrodynamic model was implemented to characterize salinity variations in time and space. The numerical simulations were carried out using the finite element numerical model 2DEF [30–32], which was developed at the Department ICEA of University of Padova and widely applied and validated in the Venice Lagoon [33–37]. The model solves the two-dimensional shallow water equations in a suitable form to deal with flooding and drying processes in very irregular domains [31]. The integration in space uses a semi-implicit staggered finite element method [38] whereas the integration in time is made through a semi-implicit scheme. The horizontal discretization of the domain is obtained using an unstructured triangular mesh. Water levels are computed at the nodes of the grid, while depth integrated velocities are computed at the center of each triangular element [39].

The model can be also applied in 3D baroclinic mode (3DEF model), i.e., using the same horizontal grid of the 2D model, with the water column discretized in layers of variable thickness [40,41]. Water temperature and salinity are transported solving the 3D advection-diffusion equation [42]. The formulation of the 3DEF model is particularly suitable for simulating hydrodynamics, salinity transport and mixing in very shallow tidal environments. Allowing the use of very thin layers near the surface, suitable resolution can be achieved around the pycnocline, even in cases of strong vertical density gradients.

The 2DEF and 3DEF numerical models were used in sequence to simulate tidal hydrodynamics and salinity displacements in the project site. For 2DEF simulations, a mesh with about 83,600 grid points (nodes) and 160,600 triangular elements was used, including the whole Venice lagoon and a portion of the Northern Adriatic Sea (Figure 4). The resolution of the grid was greatly variable, and it was very refined in the project site where sides of triangles are <10 m. Lagoon bathymetry data were the same used in previous studies [35,43], except for the area of the project site where more detailed data acquired within the Lagoon Refresh project were available, while the 2DEF simulations were forced by imposing the tidal signal at the sea boundary and the time-varying wind blowing on the whole lagoon. The wind shear stress coefficient was the same as in previous validation studies [33,34].

The 3DEF model was applied to a sub-domain of the 2DEF (Figure 4), and it was forced by tidal levels obtained by 2DEF simulation along the southern boundary of the domain (the blue line in Figure 4) and by wind. Boundary conditions included discharges of the small rivers entering the lagoon and inflows from the Sile River through the water intake structure which was built within the Lagoon Refresh project.

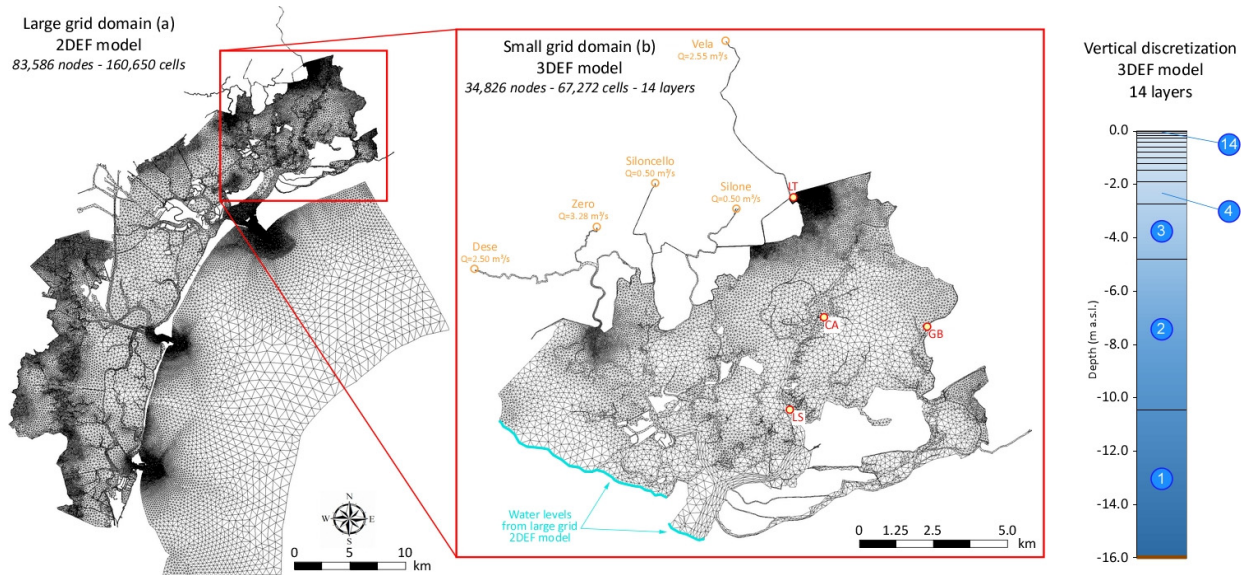


**Figure 4.** Unstructured triangular meshes used for model simulations; (a) domain of the whole Venice lagoon used with the 2DEF model (83,586 nodes and 160,650 triangular cells); (b) sub-domain of the northern lagoon used with the 3DEF model (34,826 nodes and 67,272 triangular cells, 14 layers). Tidal gauge locations (Le Trezze-LT, Grassabò-GB, Canal Ancora-CA e Le Saline-LS stations) are depicted.

Correct definition of salinity initial conditions in the model domain is critical for the 3DEF density driven simulations. Each simulation started from a salinity initial distribution derived from the available field measurements in the lagoon, and the model was run for a suitable start-up time interval (about 5 days) before the analysis period. The calibration of the model consists of the tuning of the parameters and coefficients involved in the simulated processes until the best possible agreement between measured and modeled data is obtained.

Different scenarios were performed (Table 2): for a period including the CTD campaign of 16 April 2018 in ante operam conditions of absence of flow; for a period including the CTD campaign of 23 June 2020 with a flow rate of 300 ls<sup>-1</sup>. During both campaigns, water level and current data were also acquired, by means of existing tidal gauges belonging to the ISPRA Real Time Tidal Gauge Network of the Lagoon of Venice (Grassabò-GB, Canal Ancora-CA e Le Saline-LS stations) and by temporary tidal gauge placed in the study site (Le Trezze-LT) (Figure 4); moreover, ADCP measurements were collected with a boat repeatedly navigating through four transects during the whole tidal cycle (ebb and flood). With an accurate representation of the morphology of the seabed, the only calibration parameter was the coefficient of roughness (the Strickler coefficient) that was attributed to the elements of the computational mesh with a constant value of 40 m<sup>1/3</sup> s<sup>-1</sup>. With this assumption, the model accurately reproduces both the water levels and the flow discharges measured during the campaigns.

A simulation scenario was then carried out with the calibrated model to validate modeled results with the measurements obtained in the CTD campaign of 26 February 2021 (flow rate of 1000 ls<sup>-1</sup>).

**Table 2.** Scenarios of numerical modeling simulation.

Type of Scenario	Period	Discharge Condition	CTD Campaign
Calibration	3 April–18 April 2018	0 ls <sup>-1</sup>	16 April 2018
Calibration	20 June–5 July 2020	300 ls <sup>-1</sup>	23 June 2020

Validation	23 February–10 March 2021	1000 ls <sup>-1</sup>	26 February 2021
------------	------------------------------	-----------------------	------------------

## 2.5. Data Evaluation

### 2.5.1. Moored Probes Data

To obtain a characterization over time of mean values of salinity in the area of intervention at increasing distance from the fresh water, data collected by the moored probes during periods of 14 days at the three different fresh water regimes (Table 3) were analyzed. These periods were considered long enough to include variations of tidal conditions during spring and neap tide. Temporal series of daily mean salinity and Box and Whisker plots to compare results are also presented.

**Table 3.** Periods of two weeks with different regimes of fresh water discharge, during which moored probes data were comparatively evaluated.

Phase	Discharge	Period
Post operam—fresh water flow	300 ls <sup>-1</sup>	12–25 June 2020
	500 ls <sup>-1</sup>	29 January–11 February 2021
	1000 ls <sup>-1</sup>	12–25 February 2021

### 2.5.2. CTD Profile Data

CTD profiles, obtained during the different campaigns with different discharge regimes, were analyzed to evaluate, for specific instantaneous conditions corresponding to the acquisition during field campaigns, the distribution in space and the thickness of the fresh water lens transported by the interaction of the fresh water flow and the tide inside the lagoonal water body.

Vertical profiles acquired for different positions (Table 4) chosen in the CTD local scale grid (Figure 3) at increasing distance from the input are compared.

**Table 4.** Specific positions chosen in the CTD local scale grid (Figure 3) to evaluate vertical profiles at increasing distance from the fresh water input.

Position	Distance from Input
GRD3	120 m on west direction
GRD29	105 m on south direction
GRD23	500 m on south direction
GRD10	1400 m on south direction

Particular attention was focused to evaluate the surface layer to compare CTD measures with continuous measures acquired by the moored probes and data produced by numerical modeling simulations.

### 2.5.3. Numerical Model Data

In particular, from model results, timeseries of salinity were analyzed with automated DrEAM tools [44], originally implemented for the quantitative characterization of dredging plume dynamics and here adapted to evaluate salinity temporal and spatial variations. For each node and at each vertical layer or combination of them in the domain, time series of salinity can be extracted.

Due to the shallowness of the area, in different positions of the domain as a function of the local bathymetry, the different vertical layers along the water column may experience dry conditions depending on the tidal level (H, black dashed line in Figure 5), with deeper layers drying earlier. A realistic mean value of salinity for a Surface Layer (bold



blue continuous line in Figure 5) can be obtained by evaluating the mean time series for Layers 11–14 (vertical part of the water column between the surface and  $-0.42$  m).

Statistical parameters (i.e., mean, standard deviation, standard error, etc.) useful for the quantitative characterization of the salinity variation in space can be derived integrating information over time. In particular, maps of mean salinity during the entire duration of simulation for the surface layer were calculated by evaluating for each point in the domain the mean value over time (blue dashed line in Figure 5) of the specific time series, and comparing it to the thresholds (i.e., 5–15–25), established as reference values to be achieved by the project. The extracted timeseries can be easily compared with thresholds, by identifying events (duration,  $t_i$ , Figure 5) when salinity condition is lower than specific values (e.g., 15, threshold of interest to evaluate reedbed suitability conditions).

Maps of the percentage of time when salinity is lower than a threshold can show areas with more or less stable conditions in term of mean salinity.

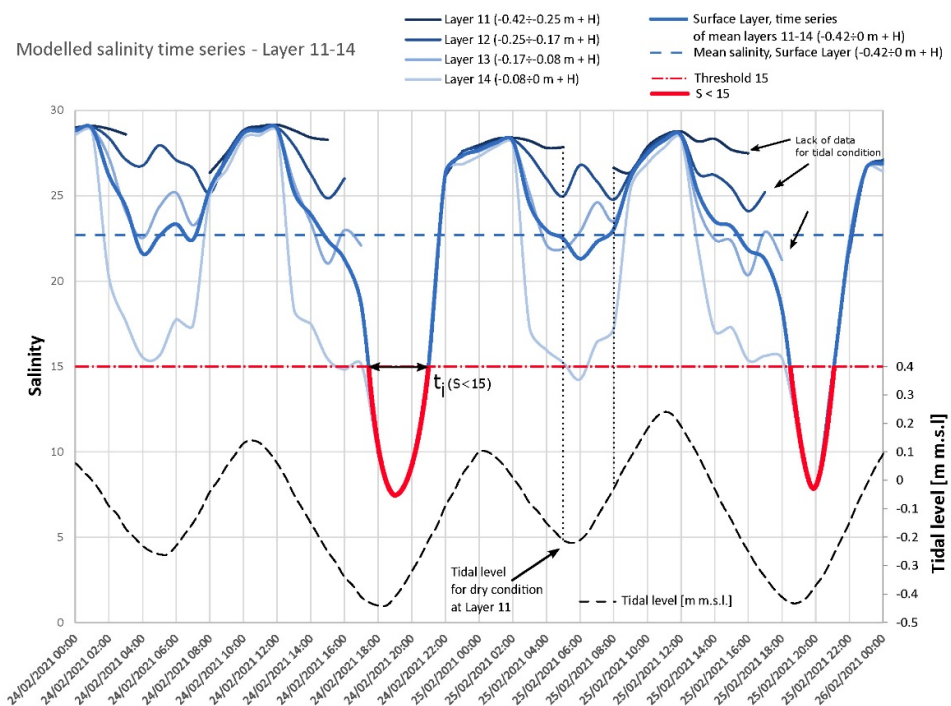


**Figure 5.** Numerical modeled time series of salinity for different vertical layers (11–14, wet or dry as a function of local bathymetry and tidal level) and their mean salinity values (Surface Layer). Identification of events (duration,  $t_i$ ) with salinity lower than a defined threshold (15). Evaluation of mean salinity values over time.

### 3. Results

#### 3.1. Moored Probes

The value of salinity changes during the day because of the tidal level and its interaction with fresh water flows (Figure 6). In ante operam conditions, with no fresh water flow (Figure 6a), the salinity fluctuates during the day in a range of 5, while, in post operam condition with a fresh water inflow of  $300 \text{ ls}^{-1}$  established after May 2020 (Figure 6b), salinity can experience sharper daily variability (up to a daily range of 30). Overall, the daily minimum salinity occurs during the low tide at the end of the ebb phase.

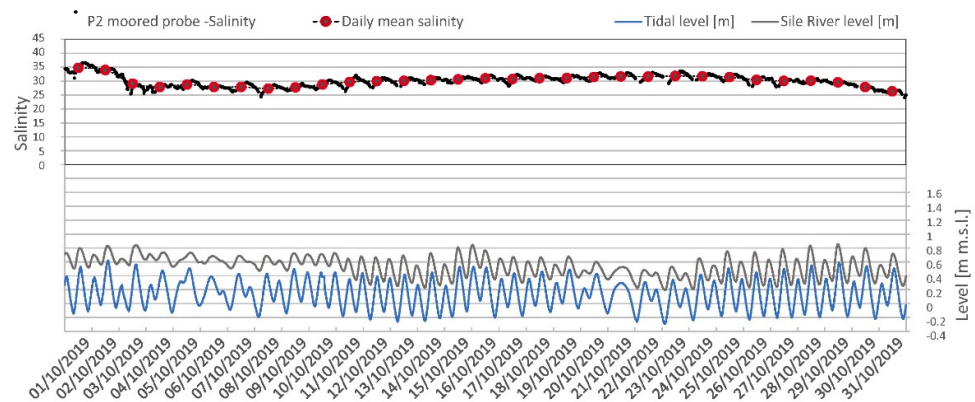
Moreover, during flood conditions, corresponding to higher level of the Sile River (Figure 6b, bold grey line, 7–10 June 2020) and stronger difference between Sile River level

and lagoon mean level, salinity undergoes long lasting drops due to the overflow of the fresh water from the river (spillway present close to the Project opera) into the lagoon.

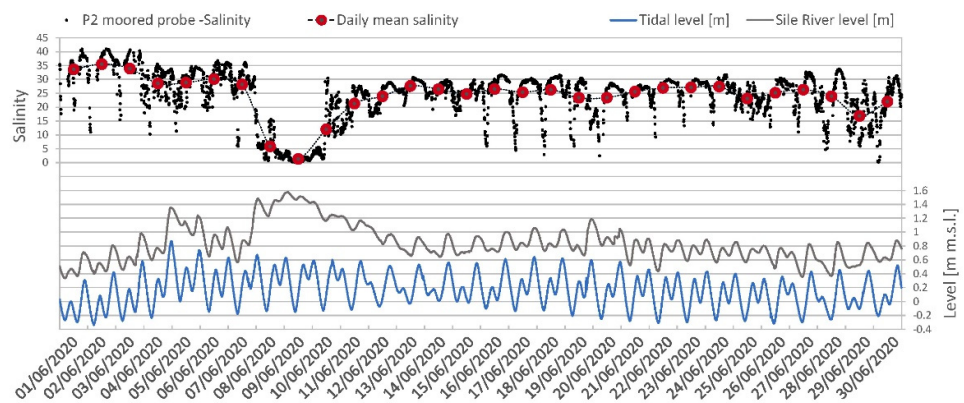
Despite the minor daily fluctuations, in the ante operam, monthly averaged salinity showed a clear seasonal pattern, with higher values in summer (close to 30) and lower salinity in late autumn/early winter (Table 5). The low salinity values, in the ante operam, were related to the several overflow events occurred in that period.

After May 2020, a fresh water flow was established and progressively increased from 300  $ls^{-1}$  up to 1000  $ls^{-1}$  reached in February 2021.

Looking at the results relative to each probe, the mean values of salinity is decreasing with the increasing of discharge. In the analyzed periods (Table 3), data from the probe closer to the fresh water input (P1) decreased from a mean value higher than 20 (discharge 300  $ls^{-1}$ ) to mean salinity lower than 5 (1000  $ls^{-1}$ ). Similarly, at the probe P2, salinity decreased approximately from 25 to 15. Minor variations occurred in the probe P3, located at a major distance from the fresh water input.



(a)



(b)

**Figure 6.** Data of salinity (10 min of frequency) registered in 10/2019 ((a), ante operam condition) and June 2020 ((b), post operam condition) in P2 moored probe. Comparison with lagoon tidal level and Sile River level data is reported to show the complex trend of salinity as a function of the tidal level and its interaction with fresh water flows.

**Table 5.** Statistics of monthly mean values of salinity before the establishment of a regular fresh water flow (May 2020) acquired by P2 moored probe installed in the middle of the area of interest.

Period	Mean Salinity	Standard Deviation
May 2019	21.96	3.95
June 2019	31.29	5.78
July 2019	33.69	3.79
August 2019	29.43	1.58
September 2019	32.34	4.03
October 2019	31.46	2.01
November 2019	21.57	5.60
December 2019	16.72	3.35
January 2020	17.16	2.15
February 2020	21.45	2.97
March 2020	24.49	3.08
April 2020	32.85	4.40

The differences among the probes constantly increased with the increasing of the fresh water input rate (Figure 7). With 300 l/s regime, all sites have comparable variation around the median value and the influence of fresh water is limited at the P1 and P2 sites. Increasing the discharge, the influence of the fresh water increases as expected: measures at P1 and P2 sites show an increase in lower salinity values. Finally, with 1000 l/s regime, the decrease in salinity and a marked gradient becomes a consolidated result: P1 is almost always below 5, P2 shows a very large variation in salinity, while P3 has a low variation around the median value (25.6). The above-mentioned patterns are confirmed by the time series, acquired from the three moored probes, of daily mean salinity for the period between 12–25/02/2021 with discharge of fresh water of 1000 l/s (Figure 8).

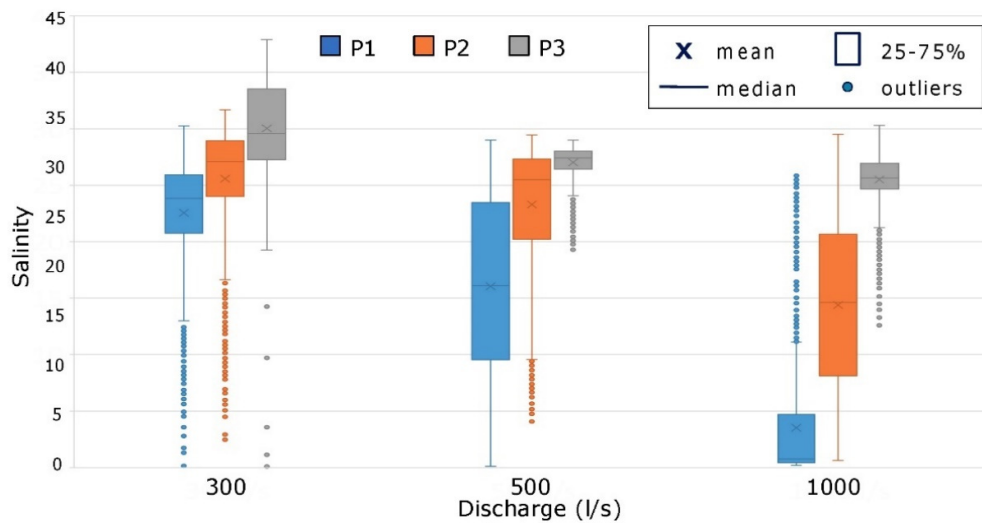


**Figure 7.** Box and Whisker plots relative to three periods of two weeks with different regimes of fresh water discharge are compared. Data relative to the three positions (P1-P2-P3) are reported.

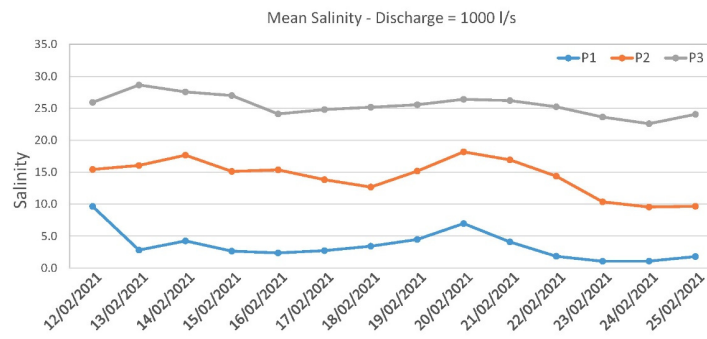


**Figure 8.** Daily mean salinity acquired from moored probes for the period 12–25 February 2021 with discharge of fresh water of 1000 l/s<sup>-1</sup>.

Differences of mean salinity between the different locations along the transect with increasing distance from the fresh water input are clearly reported. Values lower than 5 are registered close to the input (P1 probe), values around 15 are registered in the middle of the area (P2 probe) and values around 25 are registered outside the structures (P3 probe).

3.2. CTD Profiles

The spatial distribution of salinity, captured during the CTD campaign of 16/04/2018 before the fresh water input, shows the almost complete absence of a gradient of salinity, with values between 26.7 and 31.5 (Figure 9a).

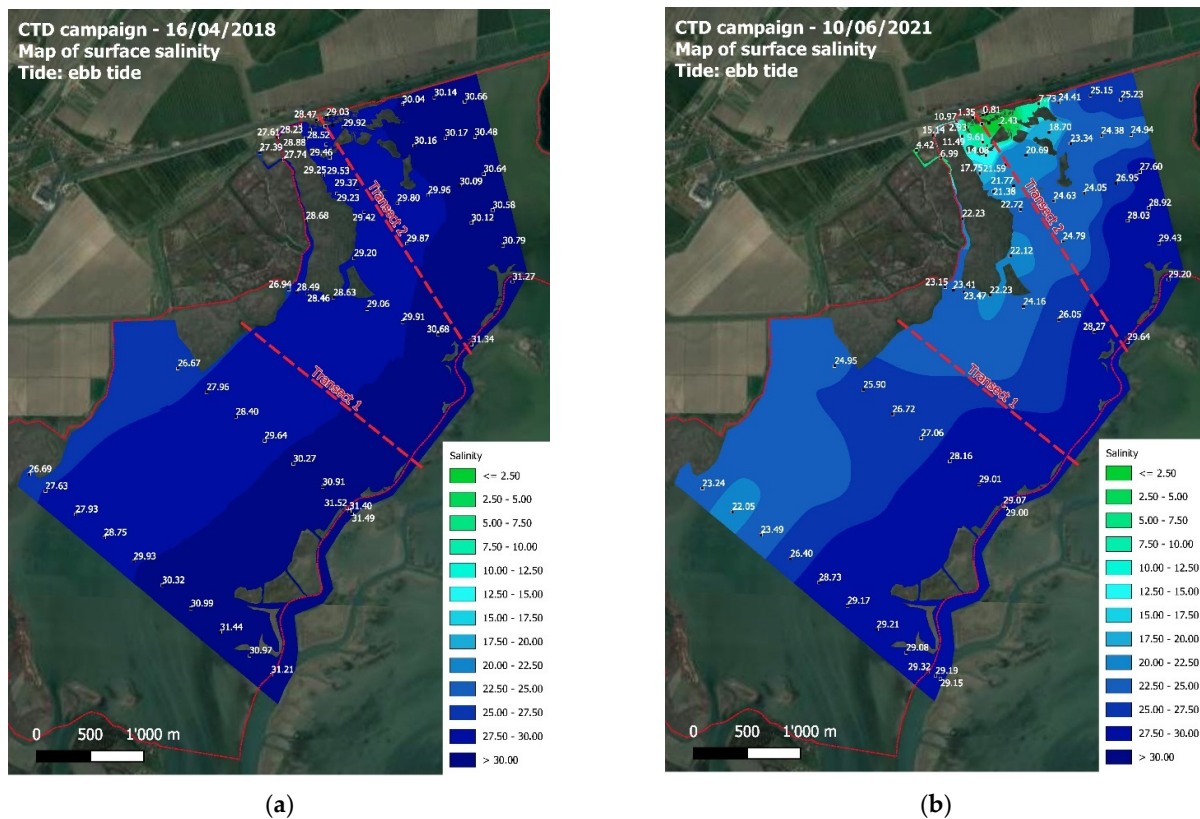


**Figure 9.** Map of Kriging interpolation performed on results of CTD campaigns: (a) campaign of 16 April 2018 with no fresh water input; (b) campaign of 10 June 2021 with a discharge of 1000 l/s<sup>-1</sup>. In both maps, the surface layer (0–30 cm) is reported.



The established gradient within the area of interest, with discharge of 1000 ls<sup>-1</sup> can be verified analyzing the results of the CTD campaign of 10 June 2021 (Figure 9b).

Comparing the condition before fresh water flow (CTD campaign of 16 April 2018) and after the consolidated discharge of 1000 ls<sup>-1</sup> (10 June 2021), the results show a strong reduction of surface salinity within a distance of 500 m from the fresh water input along transect 2, with salinity lower than 5 within 200 m and salinity lower than 15 within 400 m (Figure 10).

To investigate the changes in vertical distribution of salinity with increasing discharges as a function of the distance from the input of fresh water, vertical profiles were collected during the CTD campaigns respectively in ante operam conditions (16 April 2018, AC) and post operam conditions (10 June 2021, PC) at increasing distance from the input (GRD3, GRD29, GRD23, GRD10) (Figure 3 and Table 4).

Before fresh water input, the vertical profile is homogeneous, with constant values around 28–30 for each position. During the post operam phase with discharge of 1000 ls<sup>-1</sup>, in positions closer to the fresh water input (around 100–120 m, GRD3 and GRD29) a strong vertical stratification can be found with a sharp reduction of salinity for depth between 20 and 30 cm that corresponds to a fresh water lens floating on heavier salt water (Figure 11).

Homogeneous vertical profile can be found only at distances greater than 500 m (GRD23-GRD10), but mean salinity value is definitely lower (with values of 22 and around 25).

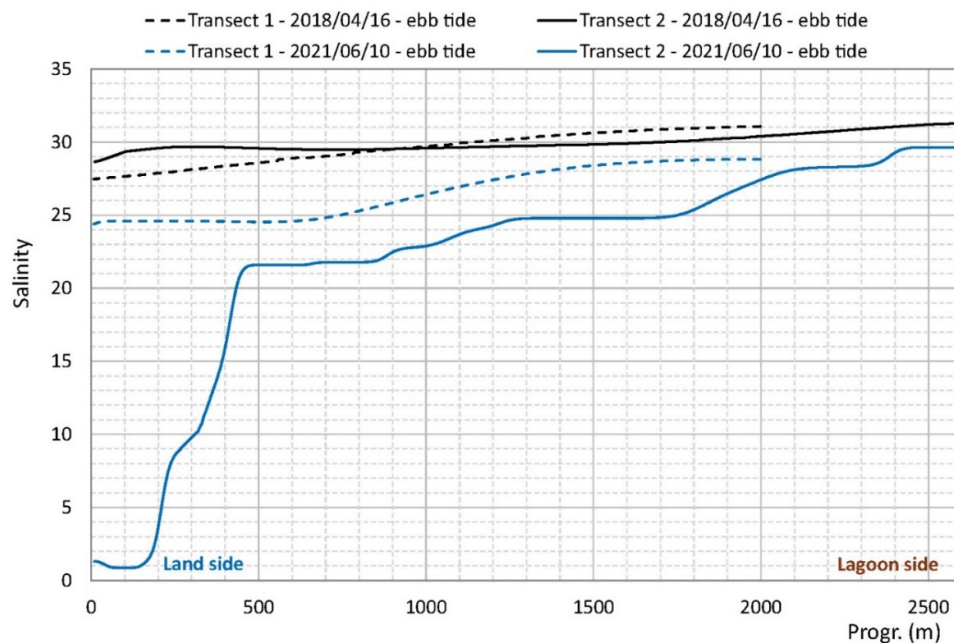


**Figure 10.** Variation of mean surface salinity along spatial transect 1 and 2 comparing the two CTD campaigns without flow (16 April 2018, black lines) and with a discharge of 1000 ls<sup>-1</sup> (10 June 2021, blue lines).

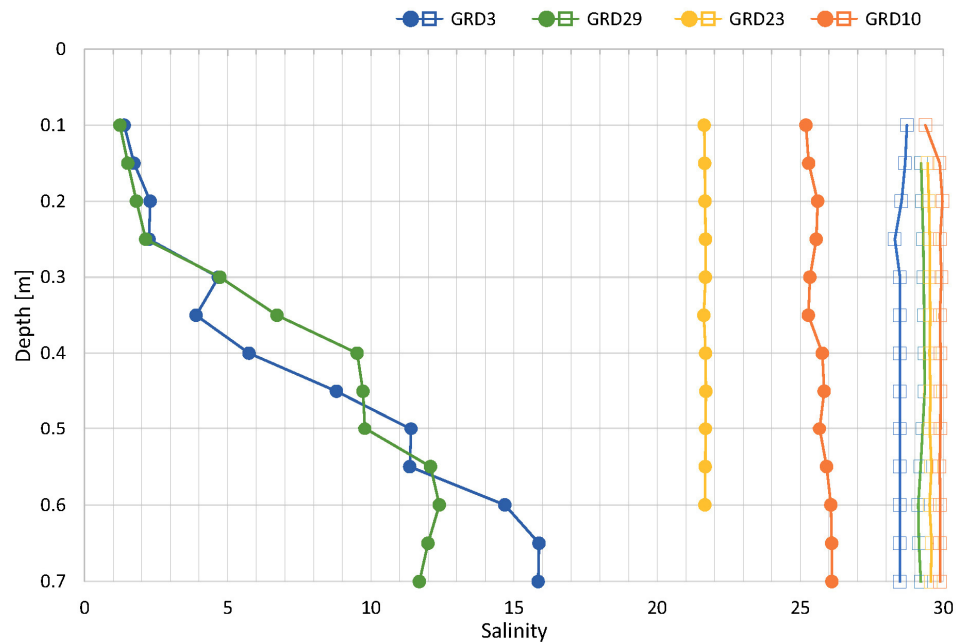


**Figure 11.** Vertical profiles of salinities at four different stations collected during two CTD campaigns in ante operam condition (open square symbols, 16 April 2018) and post operam condition (closed circle symbols, 10 June 2021), respectively. The color-coded stations GRD3, GRD29, GRD23 and GRD10 are located at increasing distance from the freshwater inputs, see Table 4 and Figure 3.

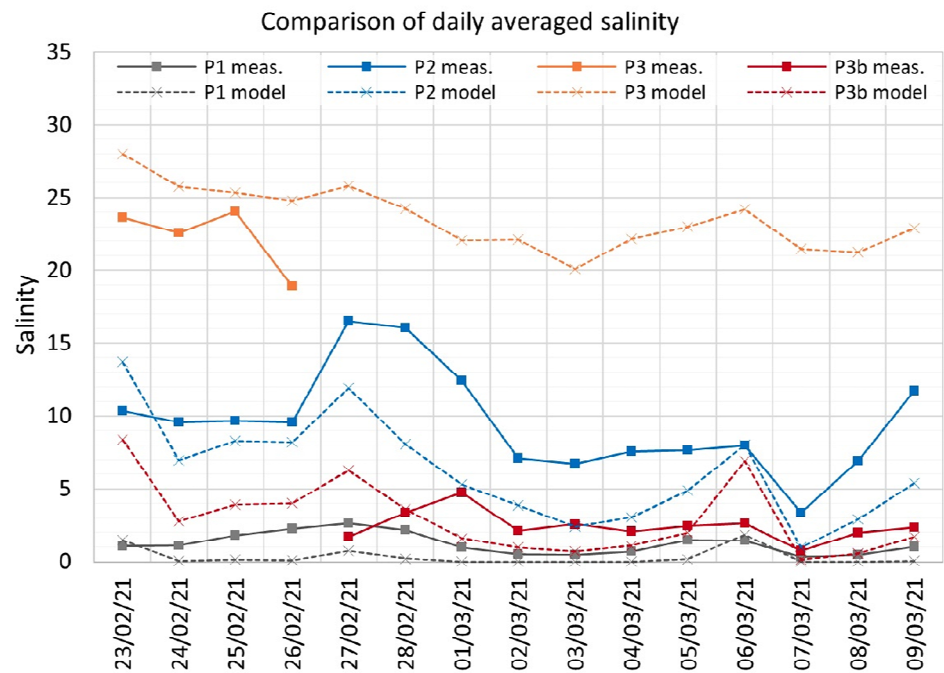
### 3.3. Numerical Modeling

The numerical study was carried out for evaluating model performances, by comparing computed salinity and observations by the moored probes and data collected during the CTD surveys, and for investigating in detail the horizontal and vertical displacement of the fresh water in the study area, during the different phases of the tidal cycle (flood tide and ebb tide). For this purpose, a 15-day simulation was run to reproduce the period 23 February 2021–10 March 2021, when the average fresh water discharge introduced in the lagoon from the Sile river was maintained at  $1000 \text{ ls}^{-1}$ .

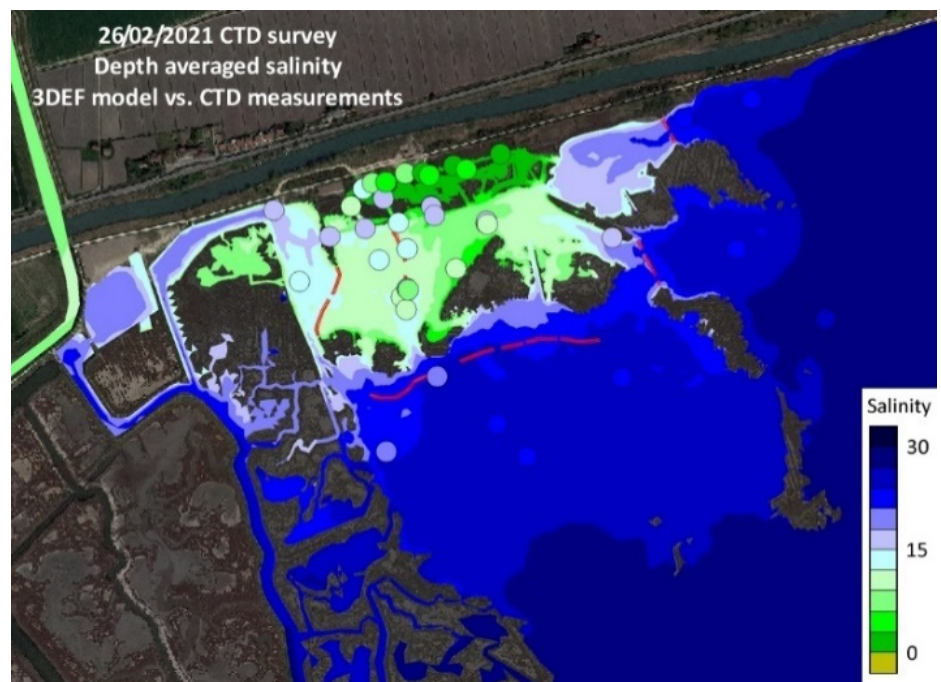
#### 3.3.1. Model Performance

The comparison of modeled and measured salinity is satisfactory both for the moored probes data and the CTD samples. Despite the complexity of the flow field, which is driven by tide, wind and density differences and is strongly influenced by the complicated morphology of the area, model results compare favorably with the measures. Daily averaged salinity trend at the moored probes is very close to measures and well represents the persistence of the strong horizontal salinity gradient that is established between the point where the fresh water is introduced and the open part of the lagoon (Figure 12a). Comparison with the CTD samples also demonstrates that model results can reproduce the actual flow paths and can give a realistic representation of the fresh water spreading in all the study area (Figure 12b).





(a)



(b)

**Figure 12.** 23 February–9 March 2021 simulation. (a) Comparison of daily averaged salinity computed and measured at moored probes; (b) map of depth-averaged salinity obtained by model results and by CTD measurements of 26 February 2021.

The variability of the salinity in space, that is at different distances from the fresh water source, and in time, that is at different times during the tidal cycle, is well illustrated

by the plots in Figure 13, representing calculated salinity at the P1-P2-P3 moored probes. Plots refer to the last four layers of the vertical model discretization (layers 11–14), which approximately represents the 40 cm surface layer of the water column (see Figure 4). It can be observed that in the point closer to the fresh water source (P1) the average salinity remains around zero, whereas at the farthest point (P3) it varies around 20–25. In the intermediate point (P2), the salinity assumes intermediate values as expected. However, it is evident that in P2 the fluctuations in salinity due to tidal variations are much more pronounced than in the other two points, since salinity approximately varies between 0 and 20 at each tidal oscillation. Basically, as will be better explained later, the areas located halfway between the stations P1 and P3 show the greatest variations of salinity in time.

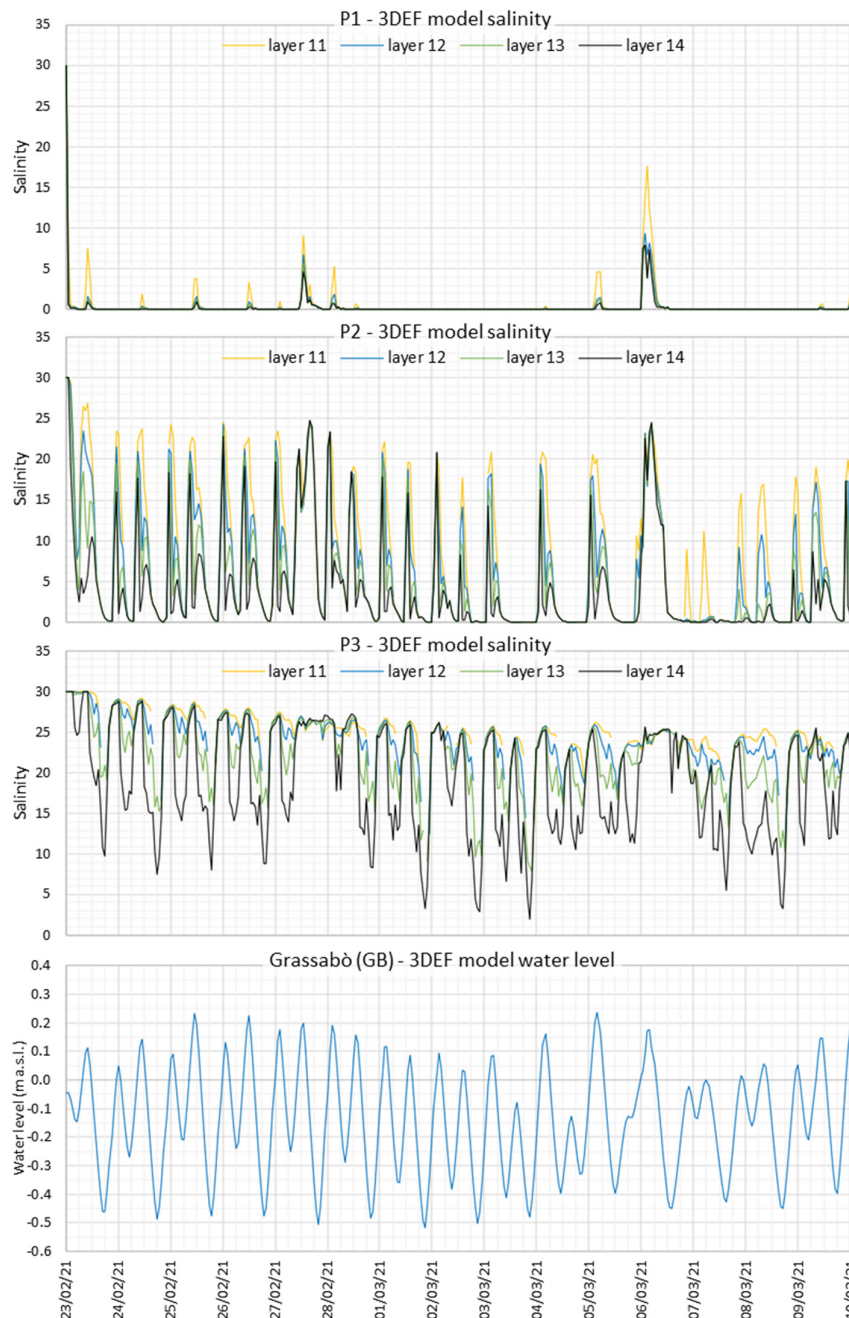


**Figure 13.** 23 February–9 March 2021 simulation. Salinity in the position of P1-P3 moored probes calculated by the model for the surface layers (11–14).

### 3.3.2. DrEAM Tool

Applying the DrEAM tool, a map of mean salinity during the entire duration of simulation (23 February–10 March 2021) was calculated for the Surface Layer evaluating for each point in the domain the mean value over time of the specific time series (Figure 14). This map was produced by identifying discrete classes of values of salinity (0–5, 5–15, 15–25, >25) and clearly shows the extension of areas with the new established condition as a consequence of the interaction between the fresh water flow and the tidal oscillation. In particular, an area of about 8 ha has a mean salinity value lower than 5, an area of about 34 ha has a mean salinity value lower than 15 and an area of about 96 ha has a mean salinity value lower than 25.

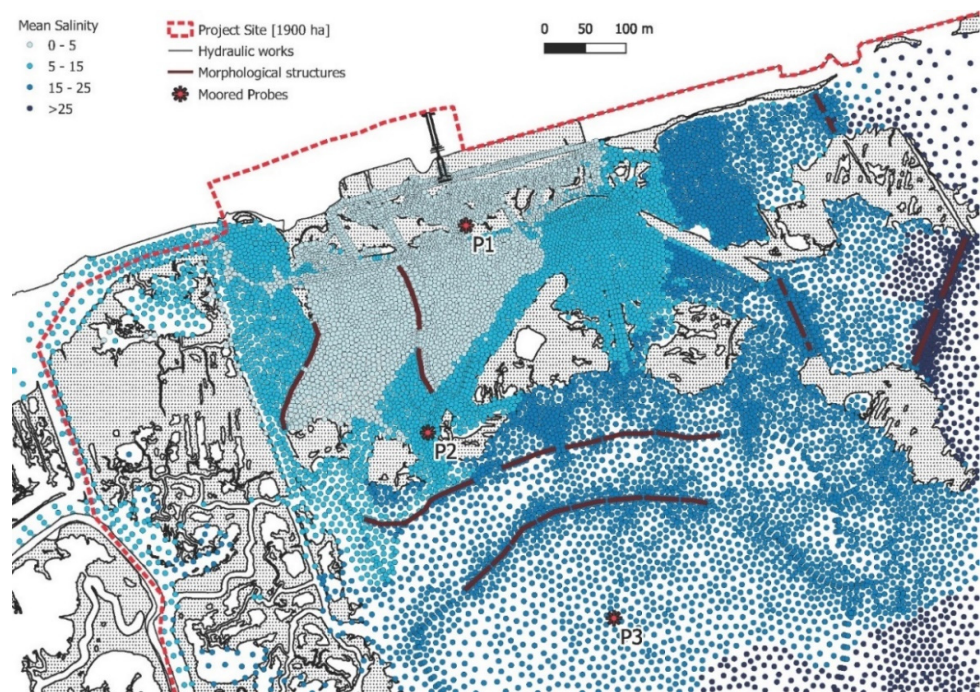


**Figure 14.** Maps of salinity distribution, evaluated as the mean value computed by the model within the vertical layers 11–14 in each node of the domain, for the period 23 February–10 March 2021, with a discharge of  $1000 \text{ ls}^{-1}$ .

Comparing the mean values (respectively around 5 for P1, 15 for P2 and 25 for P3, Figure 8) for daily time series and the values of mean salinity in their positions in the map of synthesis of numerical modeled data reported in Figure 14, it can be stated that these probes well represent their surroundings.

A map of the standard error of mean salinity during the entire duration of simulation (23 February–10 March 2021) was calculated for the surface layer, by evaluating for each point in the domain the ratio between the standard deviation and the root of the number of elements in the specific time series (Figure 15). With a  $1000 \text{ ls}^{-1}$  discharge, the area closer to the fresh water inlet (near P1 site with mean salinity from 0 to 5) and the farthest one (near P3 site with mean salinity from 15 to 25) are less variable in terms of salinity, while, in the transitional area, where fresh water and marine water mix themselves according to tidal cycles and the Sile river level, the maximum mean variability is detected. The model simulates a detailed spatial-distributed picture of what was already reported, by means of Box and Whisker plots for the three positions (P1–P2–P3) in Figure 7, in term of variations of salinity in space. Mean variability at the right side of the hydraulic structure is higher than at the left side also because bathymetry is very shallow (presence of tidal flats around salt marshes). Standard error, instead of standard deviation, was adopted as a



measure of variability to consider in the calculation of the different amounts of available data related to water depth and the number of vertical layers.

A map of the percentage of time with condition of mean salinity lower than 15, computed using the DrEAM tool within the vertical layers 11–14 in each node of the domain, was produced (Figure 16).

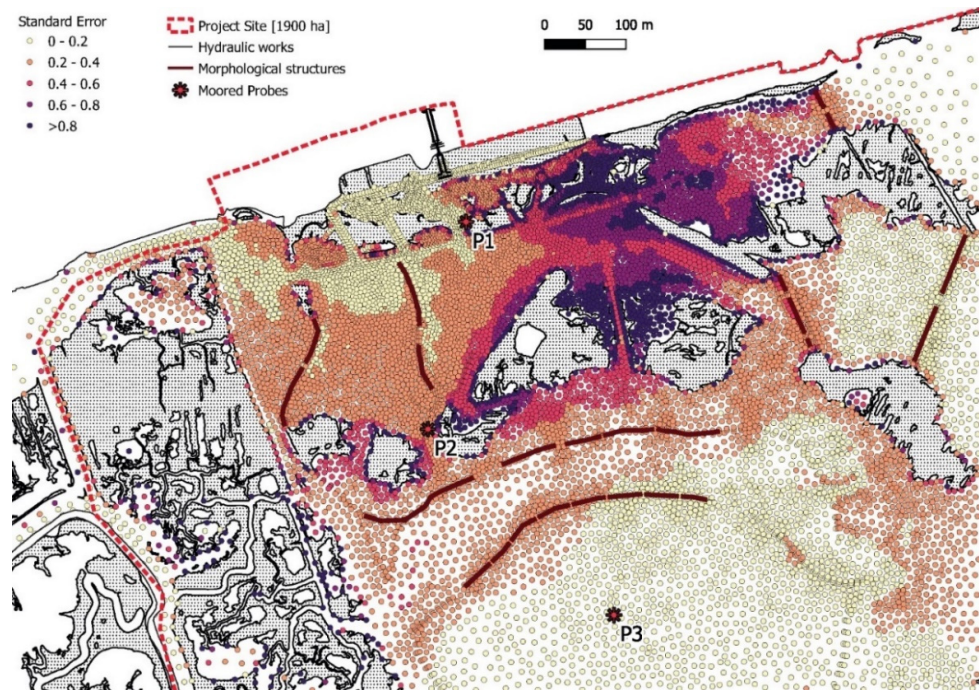


**Figure 15.** Maps of standard error of salinity values computed by the model within the vertical layers 11–14 in each node of the domain, for the period 23 February–10 March 2021, with a discharge of 1000 ls<sup>-1</sup>.

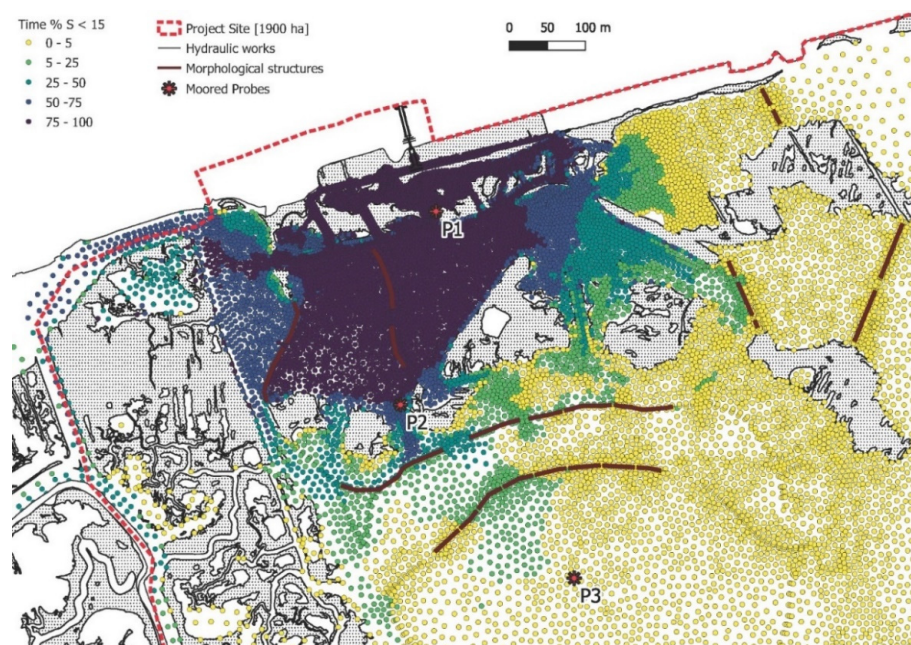


**Figure 16.** Maps of percentage of time with condition of salinity, evaluated as the mean value computed by the model within the vertical layers 11–14 in each node of the domain, <15 (condition for reedbed suitability).

In the area in front of the fresh water inflow and delimited by the morphological structure, about 8 ha, the condition of mean salinity lower than 15 can be considered to be stable, being in place for 75%–100% of time. Correspondingly, an area of about 15 ha undergoes a mean salinity lower than 15 for at least 50% of time.

#### 4. Discussion

Depending on the nature (hydraulic works, natural connection) and the characteristics of their connections with the sea, their watersheds or surrounding rivers, shallow coastal lagoons can exhibit very significant spatial and temporal heterogeneity in both salinity and water level. The importance of implementing different monitoring strategies to understand the hydrosaline functioning of these lagoons is reported in the recent literature [11].

In the planning phase of restoration projects, the objectives should be identified, along with specific indicators to measure project progress [21]. Considering the objectives of the Life Lagoon Refresh project, to restore the typical salinity gradient on a transitional environment within the Northern Venice Lagoon, and the spatial and temporal complex variability of the salinity to be investigated, a monitoring strategy of salinity with different tools was developed.

The effectiveness of the conservation actions was preliminarily investigated and then verified through the combined implementation of environmental monitoring and numerical modeling. In particular, in this case study, despite the small size of the area, a very high effort of investigation was adopted, considering that:

- the restoration of the saline gradient, main objective of the project, required a precise quantitative analysis;
- the high spatial variability, induced by the realization of the intervention with the introduction of a fresh water flow, and temporal variability on a short and medium scale, due to the interaction of the tide and the seasonal variability of the boundary conditions, required a detailed description with adequate resolution in time and space;
- each tool has different features and only an integrated approach can identify pros and cons and define a combined, effective and efficient strategy;
- the consolidated small-scale approach should be robust and applicable to all scales.

Looking at moored probes, the recording of continuous data is particularly important in the presence of high variability in time. Continuous probes allow to detect fluctuations related to the tidal level and phase. In general, minimum salinity values are observed in conditions of ebb tide, in which the fresh water flow encounters a decreasing obstacle to propagation and a decreasing amount of water, while in flow tide condition, salinity is higher due to the increasing tidal level that holds the fresh water front near the input.

Continuous data are important not only to analyze short-term fluctuations, but also to have a reliable average value on a longtime scale (monthly/annual), free from the randomness of the sampling moment or from the systematic selection of certain biased sampling conditions (e.g., accessibility of certain areas only with high tidal condition).

The presence of three probes made it possible to highlight the restoration of a gradient in space at an increasing distance from the fresh water input. An interesting aspect that emerged is the differentiation of the three probes with more defined conditions corresponding respectively to a stronger influence of fresh water input for the nearest position (P1) and a stronger influence of tide for the outermost position (P3), while more variable conditions were collected for the intermediate station (P2). Continuous measurements allow the acquisition of critical data for the development, calibration and validation of hydrodynamic models that can provide additional information on the hydro-saline functioning of lagoons [11,15,45–49].

The results obtained from the campaigns with CTD profiles allow for highlighting the spatial variability in a precise instant of time and confirm the presence of a marked

gradient in space. The limitations of this approach are mainly two: CTD survey returns an instantaneous picture, with values possibly not representative of average conditions but strongly influenced by the sampled instant of tide; in conditions of low tide, the limited accessibility by boat of certain shallow and confined areas, particularly interesting for the reedbed suitability, prevents the characterization of these areas and limits the possibility to prove with measures the establishment of the desired suitable conditions.

On the other hand, spatially-distributed profiles are also particularly useful for the validation of numerical modeling results in terms of spatial distribution of salinity patterns [11,15].

Moreover, CTD profilers allow the characterization of spatial variability of salinity not only in term of horizontal patterns but also in term of vertical distribution and possible stratification. The analysis of the results indicates, near the input zone, a stratification in the first 30 cm where water depth is lower than one meter, probably related to reduced hydro-dynamism due to the absence of wave motion and weak tidal currents. Differently, a lower stratification was detected at increasing distance from the input, where lower values of salinity homogeneously established on the vertical profile as a consequence of the fresh water inflow.

Depending on the specific objectives of the monitoring strategy, it is necessary to evaluate whether to consider surface layers or rather average conditions on the vertical. In the specific case, the surface layers are of greater interest in the study of fresh water propagation and in the detailed physical description of the dynamics of fresh and salt waters while evaluations in terms of average salinity are more interesting in relation to the verification of the conditions of suitability for the development of reeds. Specific assessments on deep layer conditions could be also interesting for detailed studies related to the interfaces between water column and soil, in relation to biological considerations on the rooting of transplants, envisaged as a conservation action by the project.

Finally, looking at the numerical tool, a calibrated and validated numerical model allows to reproduce both the singularities (e.g., zones of river inflow if well implemented in the model) and general patterns and provides reliable results without the need for a strong monitoring effort in terms of density of continuous acquisition and/or repeated distributed surveys (probes and CTD).

On the other hand, the model provides an estimate of the value, not a direct measure. Especially in the case of use on the large-scale, results are strongly influenced by the quality of the information related to the forcing factors (e.g., discharge of fresh water inputs) and by the initial and boundary conditions (e.g., average salinity of the lagoon). Incorrect initial and boundary conditions could lead to errors in the estimation of the absolute value of salinity, even if a correct description of the spatial patterns and temporal variations of the dynamics is reported.

However, the results of the numerical model allow to integrate the different aspects and to maximize the information on all spatial and temporal scales, extracting synthetic indicators. In the presented case study, the production of maps of the synthesis of the main statistics was used to estimate the area in which the results were achieved in terms of average salinity and percentage of time of permanence under certain thresholds of mean salinity.

With this approach, the model can be used to identify homogeneous areas within the domain of interest, both in the preliminary phase of the definition of the monitoring strategy or in a possible optimization phase, where continuous probes can be installed/moved to acquire data truly representative of homogeneous areas. Moreover, homogeneous areas of possible interest are characterized not only by average conditions but also by a certain variability. The presented results specifically indicate a pattern of variability that does not follow a gradient but that identifies an intermediate transition zone between areas near the inflow where proper fresh water conditions are established, and internal lagoon dominated by tidal oscillation and influenced by the sea.



As already reported, the integration of results obtained with the three different tools, and in particular the statistical analysis of continuous time series compared with the maps produced through the application of DrEAM to numerical results, permitted to verify the achievement of the project objective in terms of the extension of areas with average salinity lower than specific thresholds and in term of stability in time of the reached conditions.

Continuous and periodic monitoring strategies have variable operational costs, considering both the acquisition of instruments and the human resources required to carry out the measurements (periodic measurement campaigns, regular maintenance of continuous probes and flowmeters, etc.). An efficient and sustainable monitoring of the hydro-saline dynamics of lagoons must, therefore, be a compromise between all these different criteria [11]. Future research could be the optimization of the monitoring strategy to maximize results minimizing the monitoring effort.

## 5. Conclusions

The main goal of the Life Lagoon Refresh (LIFE16NAT/IT/000663) project is to restore the typical salinity gradient on a transitional environment in the Northern Venice Lagoon, improving its conservation status and biodiversity through different conservation actions. The effectiveness of these actions was preliminarily investigated and then verified through the combined implementation of environmental monitoring and numerical modeling. The characterization in time and space of salinity variations was obtained by the acquisition of continuous data (moored salinity probes), field campaigns (CTD probes) and numerical modeling. These different tools were synergically used to highlight the establishment of a stable average condition of salinity gradient in the different project areas. Different results were illustrated and compared. Among these, the most significant are the statistics of the time series of salinity acquired in fixed positions, instantaneous results of CTD campaigns distributed in space, integrations over time of modeling results to include the interaction between tide and a regular fresh water input.

Through the different results, the achievement of the project objective in recreating a consolidated salinity gradient was demonstrated through quantitative indicators. The characterization of the variability in the intermediate transition zone between fresh water conditions (river input) and lagoon/marine conditions was also reported.

**Author Contributions:** Conceptualization, A.F., E.P., M.C., R.B.B., B.M., D.C. and A.B.; data curation, A.F., E.P., M.C. and D.C.; formal analysis, A.F., E.P., M.C., B.M. and D.C.; funding acquisition, R.B.B., P.P., M.L., V.V., A.S. and A.B.; investigation, A.F., E.P., M.C., B.M., D.C. and A.B.; methodology, A.F., E.P., M.C., R.B.B., B.M., D.C. and A.B.; project administration, R.B.B. and A.B.; resources, R.B.B., P.P., M.L., V.V., M.F. and A.B.; software, A.F. and D.C.; supervision, R.B.B., M.F. and A.B.; validation, A.F.; visualization, A.F., E.P., M.C. and D.C.; writing—original draft, A.F., E.P., M.C., B.M., D.C. and A.B.; Writing—review and editing, A.F., E.P., M.C., R.B.B., F.C., F.O., S.S., P.P., M.L., L.M., A.S. and A.B. All authors have read and agreed to the published version of the manuscript.

**Funding:** This research was funded by the European Union’s LIFE program financial instrument 2014–2020 (grant LIFE16 NAT/IT/000663—LIFE Lagoon Refresh, which contributes to the environmental recovery of a Natura 2000 site, SCI IT3250031—Northern Venice Lagoon).

**Institutional Review Board Statement:** Not applicable.

**Informed Consent Statement:** Informed consent was obtained from all subjects involved in the study.

**Data Availability Statement:** The data presented in this study are available on request from the corresponding author. The data are not publicly available.

**Conflicts of Interest:** The authors declare no conflicts of interest.

## References

1. Pérez-Ruzafa, A.; Marcos, C.; Pérez-Ruzafa, I. Mediterranean coastal lagoons in an ecosystem and aquatic resources management context. *Phys. Chem. Earth* **2011**, *36*, 160–166. <https://doi.org/10.1016/j.pce.2010.04.013>.
2. Cataudella, S.; Crosetti, D.; Massa, F. Mediterranean coastal lagoons: Sustainable management and interactions among aquaculture, capture fisheries and the environment. In *FAO Studies and Reviews General Fisheries Commission for the Mediterranean*; Food & Agriculture Organization of the United Nations (FAO): Rome, Italy; 2015; p. 293.
3. Reizopoulou, S.; Simboura, N.; Barbone, E.; Aleffi, F.; Basset, A.; Nicolaidou, A. Biodiversity in transitional waters: Steeper ecotone, lower diversity. *Marine Ecol.* **2014**, *35*, 78–84. <https://doi.org/10.1111/maec.12121>.
4. Tagliapietra, D.; Sigovini, M.; Volpi Ghirardini, A. A review of terms and definitions to categorize estuaries, lagoons and associated environments. *Mar. Fresh Water Res.* **2009**, *60*, 497–509. <https://doi.org/10.1071/MF08088>.
5. Smyth, K.; Elliott, M. Effects of changing salinity on the ecology of the marine environment. In *Stressors in the Marine Environment: Physiological and Ecological Responses; Societal Implications*; Solan, M., Whiteley, N., Eds.; Oxford University Press: Oxford, UK, 2016; ISBN 13 9780198718826.
6. Scapin, L.; Zucchetto, M.; Bonometto, A.; Feola, A.; Boscolo Brusà, R.; Sfriso, A.; Franzoi, P. Expected shifts in nekton community following salinity reduction: Insights into restoration and management of transitional water habitats. *Water* **2019**, *11*, 1354. <https://doi.org/10.3390/w11071354>.
7. Le Fur, I.; De Wit, R.; Plus, M.; Oheix, J.; Simier, M.; Ouisse, V. Submerged benthic macrophytes in Mediterranean lagoons: Distribution patterns in relation to water chemistry and depth. *Hydrobiologia* **2018**, *808*, 175–200. <https://doi.org/10.1007/s10750-017-3421-y>.
8. Bellafiore, D.; Ghezzi, M.; Tagliapietra, D.; Umgiesser, G. Climate change and artificial barrier effects on the Venice Lagoon: Inundation dynamics of salt marshes and implications for halophytes distribution. *Ocean Coast. Manag.* **2014**, *100*, 101–115. <https://doi.org/10.1016/j.ocecoaman.2014.08.002>.
9. Lee, Y.J.; Lwiza, K. Interannual variability of temperature and salinity in shallow water: Long Island Sound, New York. *J. Geophys. Res.* **2005**, *110*, C09022. <https://doi.org/10.1029/2004JC002507>.
10. Nunes, A.; Larson, M.; Fragoso, C.R.; Hanson, H. Modeling the salinity dynamics of a choked coastal lagoon and its impact on the Sururu mussel (*Mytella falcata*) population. *Reg. Stud. Mar. Sci.* **2021**, *45*, 101807. <https://doi.org/10.1016/j.rsma.2021.101807>.
11. Boutron, O.; Paugam, C.; Luna-Laurent, E.; Chauvelon, P.; Sous, D.; Rey, V.; Meulé, S.; Chérain, Y.; Cheiron, A.; Migne, E. Hydro-Saline Dynamics of a Shallow Mediterranean Coastal Lagoon: Complementary Information from Short and Long Term Monitoring. *J. Mar. Sci. Eng.* **2021**, *9*, 701. <https://doi.org/10.3390/jmse9070701>.
12. Tagliapietra, D.; Volpi Ghirardini, A. Notes on coastal lagoon typology in the light of the EU Water Framework Directive: Italy as a case study. *Aquat. Conserv. Mar. Fresh Water Ecosyst.* **2006**, *16*, 457–467. <https://doi.org/10.1002/aqc.768>.
13. Zemlys, P.; Ferrarin, C.; Umgiesser, G.; Gulbinskas, S.; Bellafiore, D. Investigation of saline water intrusions into the Curonian Lagoon (Lithuania) and two-layer flow in the Klaipeda Strait using finite element hydrodynamic model. *Ocean Sci.* **2013**, *9*, 573–584. <https://doi.org/10.5194/os-9-573-2013>.
14. Zirino, A.; Elwany, H.; Neira, C.; Maicu, F.; Mendoza, G.; Levin, L. Salinity and its variability in the Lagoon of Venice, 2000–2009. *Adv. Oceanogr. Limnol.* **2014**, *5*, 41–59. <https://doi.org/10.1080/19475721.2014.900113>.
15. Ghezzi, M.; Sarretta, A.; Sigovini, M.; Guerzoni, S.; Tagliapietra, D.; Umgiesser, G. Modeling the inter-annual variability of salinity in the lagoon of Venice in relation to the water framework directive typologies. *Ocean Coast. Manag.* **2011**, *54*, 706–719.
16. Seminara, G.; Lanzoni, S.; Cecconi, G. Coastal wetlands at risk: Learning from Venice and New Orleans. *Ecohydrol. Hydrobiol.* **2011**, *11*, 183–202. <https://doi.org/10.2478/v10104-011-0040-5>.
17. D’Alpaos, L.; Carniello, L. *Sulla Reintroduzione di Acque Dolci Nella Laguna di Venezia, in Salvaguardia di Venezia e della sua Laguna, Atti dei Convegni Lincei ACL, 255, XXVI Giornata dell’Ambiente, in Ricordo di Enrico Marchi*; Accademia Nazionale dei Lincei: Rome, Italy; 2010; pp. 113–146, ISBN 978-88-218-1021-3. (In Italian)
18. Solidoro, C.; Bandelj, V.; Bernardi Aubry, F.; Camatti, E.; Ciavatta, S.; Cossarini, G.; Facca, C.; Franzoi, P.; Libralato, S.; Canu, D.; et al. Response of the Venice Lagoon Ecosystem to Natural and Anthropogenic Pressures over the Last 50 Years. In *Coastal Lagoons: Systems of Natural and Anthropogenic Change*, Hans Paerl and Mike Kennish; CRC Press: Boca Raton, FL, USA, 2010; pp. 483–511; ISBN 9781420088304.
19. Miller, J.M.; Pietrafesa, L.J.; Smith, N.P. *Principles of Hydraulic Management of Coastal Lagoons for Aquaculture and Fisheries*; FAO Fisheries Technical Paper; FAO: Rome, Italy, 1990; Volume 314, 88p.
20. Elliott, M.; Mander, L.; Mazik, K.; Simenstad, C.; Valesini, F.; Whitfield, A.; Wolanski, E. Ecoengineering with Ecohydrology: Successes and failures in estuarine restoration. *Estuar. Coast. Shelf Sci.* **2016**, *176*, 12–35.
21. Feola, A.; Bonometto, A.; Ponis, E.; Cacciatore, F.; Matticchio, B.; Canesso, D.; Lizier, M.; Volpe, V.; Sfriso, A.; Ferla, M.; et al. Ecological Engineering for transitional water restoration: Life Lagoon Refresh case study. In Proceedings of the Symposium Soil and Water Bioengineering as a Tool for Ecological Restoration at “The 12th European Conference on Ecological Restoration”, online, 7–10 September 2021.
22. Kiviat, E. Ecosystem services of Phragmites in North America with emphasis on habitat functions. *AoB Plants* **2013**, *5*, plt008. <https://doi.org/10.1093/aobpla/plt008>.
23. Umgiesser, G.; Melaku Canu, D.; Cucco, A.; Solidoro, C. A finite element model for the Venice Lagoon. Development set up calibration and validation. *J. Mar. Syst.* **2004**, *51*, 123–145. <https://doi.org/10.1016/j.jmarsys.2004.05.009>.

24. Solidoro, C.; Melaku Canu, D.; Cucco, A.; Umgiesser, G. A partition of the Venice Lagoon based on physical properties and analysis of general circulation. *J. Mar. Syst.* **2004**, *51*, 147–160.
25. Molinaroli, E.; Guerzoni, S.S.; Sarretta, A.; Cucco, A.; Umgiesser, G. Links between hydrology and sedimentology in the Lagoon of Venice Italy. *J. Mar. Syst.* **2007**, *68*, 303–317. <https://doi.org/10.1016/j.jmarsys.2006.12.003>.
26. Ghezzi, M.; Guerzoni, S.; Cucco, A.; Umgiesser, G. Changes in Venice Lagoon dynamics due to construction of mobile barriers. *Coast. Eng.* **2010**, *57*, 694–708.
27. Feola, A.; Bonometto, A.; Ponis, E.; Cacciatore, F.; Oselladore, F.; Matticchio, B.; Canesso, D.; Sponga, S.; Volpe, V.; Lizier, M.; et al. LIFE LAGOON REFRESH. Ecological restoration in Venice Lagoon (Italy): Concrete actions supported by numerical modeling and stakeholder involvement. In Proceedings of the Citizen Observatories for natural hazards and Water Management—2nd International Conference, Venice, Italy, 27–30 November 2018.
28. UNESCO. Algorithms for computation of fundamental properties of seawater. In *Unesco Technical Papers in Marine Science*; Endorsed by Unesco/SCOR/ICES/IAPSO Joint Panel on Oceanographic Tables and Standards and SCOR Working Group 51; UNESCO: Paris, France, 1983; Volume 44, 53p.
29. Lissner, J.; Schierup, H.-H. Effects of salinity on the growth of *Phragmites australis*. *Aquatic Botany* **1997**, *55*, 247–260.
30. Defina, A.; D’Alpaos, L.; Matticchio, B. A new set of equations for very shallow water and partially dry areas suitable to 2D numerical models. In *Modelling Flood Propagation over Initially Dry Areas*; Molinaro, P., Natale, L., Eds.; American Society of Civil Engineers: New York, NY, USA, 1994; pp. 72–81.
31. Defina, A. Two-dimensional shallow flow equations for partially dry areas. *Water Resour. Res.* **2000**, *36*, 3251. <https://doi.org/10.1029/2000WR900167>.
32. D’Alpaos, L.; Defina, A. Mathematical modeling of tidal hydrodynamics in shallow lagoons: A review of open issues and applications to the Venice lagoon. *Comput. Geosci.* **2007**, *33*, 476–496. <https://doi.org/10.1016/j.cageo.2006.07.009>.
33. Carniello, L.; Defina, A.; Fagherazzi, S.; D’Alpaos, L. A combined Wind Wave-Tidal Model for the Venice lagoon, Italy. *J. Geophys. Res.* **2005**, *110*, F04007. <https://doi.org/10.1029/2004JF000232>.
34. Carniello, L.; D’Alpaos, A.; Defina, A. Modeling wind-waves and tidal flows in shallow microtidal basins. *Estuar. Coast. Shelf Sci.* **2011**, *92*, 263–276. <https://doi.org/10.1016/j.ecss.2011.01.001>.
35. Carniello, L.; Defina, A.; D’Alpaos, L. Modeling sand-mud transport induced by tidal currents and wind waves in shallow microtidal basins: Application to the Venice Lagoon (Italy). *Estuar. Coast. Shelf Sci.* **2012**, *102–103*, 105–115. <https://doi.org/10.1016/j.ecss.2012.03.016>.
36. Viero, D.P.; Defina, A. Water age, exposure time, and local flushing time in semi-enclosed, tidal basins with negligible fresh-water inflow. *J. Mar. Syst.* **2016**, *156*, 16–29. <https://doi.org/10.1016/j.jmarsys.2015.11.006>.
37. Pivato, M.; Carniello, L.; Viero, D.P.; Soranzo, C.; Defina, A.; Silvestri, S. Remote sensing for optimal estimation of water temperature dynamics in shallow tidal environments. *Remote Sens.* **2020**, *12*, 51. <https://doi.org/10.3390/rs12010051>.
38. Defina, A. Numerical experiments on bar growth. *Water Resour. Res.* **2003**, *39*, 1–12. <https://doi.org/10.1029/2002WR001455>.
39. Viero, D.P. Modelling urban floods using a finite element staggered scheme with an anisotropic dual porosity model. *J. Hydrol.* **2019**, *568*, 247–259. <https://doi.org/10.1016/j.jhydrol.2018.10.055>.
40. D’Alpaos, L.; Defina, A.; Matticchio, B. Multilayer Model for Shallow Water Flows and Density Currents applied to a Lagoon in the River Delta. In Proceedings of the 11th International Conference on Computational Methods in Water Resources, CMWR’96, Cancun, Mexico, 1 July 1996.
41. Defina, A. Modelling of Tidal Flow in Very Shallow Lagoons. In Proceedings of the 11th International Conference on Computational Methods in Water Resources, CMWR’96, Cancun, Mexico, 1 July 1996.
42. Casulli, V.; Zanoli, P. High resolution methods for multidimensional advection–diffusion problems in free-surface hydrodynamics. *Ocean Model.* **2005**, *10*, 137–151. <https://doi.org/10.1016/j.ocemod.2004.06.007>.
43. Mel, R.; Carniello, L.; D’Alpaos, L. Addressing the effect of the Mo.S.E. barriers closure on wind setup within the Venice lagoon. *Estuar. Coast. Shelf Sci.* **2019**, *225*, 106249. <https://doi.org/10.1016/j.ecss.2019.106249>.
44. Feola, A.; Lisi, I.; Salmeri, A.; Venti, F.; Pedroncini, A.; Gabellini, M.; Romano, E. Platform of integrated tools to support environmental studies and management of dredging activities. *J. Environ. Manag.* **2016**, *166*, 357–373.
45. De Pascalis, F.; Pérez-Ruzafa, A.; Gilabert, J.; Marcos, C.; Umgiesser, G. Climate Change Response of the Mar Menor Coastal Lagoon (Spain) Using a Hydrodynamic Finite Element Model. *Estuar. Coast. Shelf Sci.* **2012**, *114*, 118–129. <https://doi.org/10.1016/j.ecss.2011.12.002>.
46. Umgiesser, G.; Ferrarin, C.; Cucco, A.; De Pascalis, F.; Bellafiore, D.; Ghezzi, M.; Bajo, M. Comparative Hydrodynamics of 10 Mediterranean Lagoons by Means of Numerical Modeling. *J. Geophys. Res. Oceans* **2014**, *119*, 2212–2226. <https://doi.org/10.1002/2013JC009512>.
47. Ferrarin, C.; Umgiesser, G. Hydrodynamic Modeling of a Coastal Lagoon: The Cabras Lagoon in Sardinia, Italy. *Ecol. Model.* **2005**, *188*, 340–357. <https://doi.org/10.1016/j.ecolmodel.2005.01.061>.
48. Ferrarin, C.; Ghezzi, M.; Umgiesser, G.; Tagliapietra, D.; Camatti, E.; Zaggia, L.; Sarretta, A. Assessing Hydrological Effects of Human Interventions on Coastal Systems: Numerical Applications to the Venice Lagoon. *Hydrol. Earth Syst. Sci.* **2013**, *17*, 1733–1748. <https://doi.org/10.5194/hess-17-1733-2013>.
49. Maicu, F.; De Pascalis, F.; Ferrarin, C.; Umgiesser, G. Hydrodynamics of the Po River-Delta-Sea system. *J. Geophys. Res. Ocean.* **2018**, *123*, 6349–6372. <https://doi.org/10.1029/2017JC013601>.